

OPEN

Rac1 is a downstream effector of PKC α in structural synaptic plasticity

Xun Tu^{1,2,3}, Ryohei Yasuda^{1,2,3*} & Lesley A. Colgan^{1*}

Structural and functional plasticity of dendritic spines is the basis of animal learning. The rapid remodeling of actin cytoskeleton is associated with spine enlargement and shrinkage, which are essential for structural plasticity. The calcium-dependent protein kinase C isoform, PKC α , has been suggested to be critical for this actin-dependent plasticity. However, mechanisms linking PKC α and structural plasticity of spines are unknown. Here, we examine the spatiotemporal activation of actin regulators, including small GTPases Rac1, Cdc42 and Ras, in the presence or absence of PKC α during single-spine structural plasticity. Removal of PKC α expression in the postsynapse attenuated Rac1 activation during structural plasticity without affecting Ras or Cdc42 activity. Moreover, disruption of a PDZ binding domain within PKC α led to impaired Rac1 activation and deficits in structural spine remodeling. These results demonstrate that PKC α positively regulates the activation of Rac1 during structural plasticity.

Dendritic spines of pyramidal neurons in the hippocampus undergo activity-dependent structural and functional plasticity that has been reported to be crucial for learning and memory^{1–3}. This plasticity is mediated by the coordinated regulation of complex signaling networks that transduce short-lived synaptic input into long-lasting biochemical changes to modulate the strength and structure of synapses and, ultimately, animal behavior^{4,5}.

Protein kinase C (PKC) is a family of serine/threonine kinases that have long been implicated as essential for synaptic plasticity, learning and memory. Inhibition of PKC blocks LTP induction and also disrupts the maintenance of pre-established LTP^{6,7}. In addition, pharmacologically activating PKC or overexpressing constitutively active PKC potentiates synapses and enhances learning^{8,9}. PKC exists as at least 10 isozymes that are categorized into three subfamilies: the classic isozymes (PKC α , PKC β and PKC γ), the novel isozymes (PKC δ , PKC ϵ , PKC η , and PKC θ) and the atypical isozymes (PKC ζ and PKC λ/ι). The classic PKC isozymes, ubiquitously expressed in the brain, transduce signals dependent on Ca²⁺ and diacylglycerol (DAG)^{10–13}. Recently, PKC α was demonstrated to be uniquely required for structural LTP in hippocampal dendritic spines. This specificity was defined by a four amino acid C-terminal PDZ-binding motif (QSAV)¹⁴. Evidence suggests that PKC α activity integrates neurotrophic signaling, including the activation of TrkB, with Ca²⁺ influx through NMDARs to facilitate the induction of the plasticity in dendritic spines¹⁴. However, the downstream molecular mechanisms through which PKC α facilitates structural synaptic plasticity remain unknown.

The expression of structural plasticity, through spine enlargement and insertion of additional glutamate receptors, requires actin remodeling through the regulated activity of small GTPases including Rac1, Cdc42 and Ras^{15–19}. These small GTPases are precisely coordinated across spatiotemporal domains by a complex network of GTPase accelerating proteins (GAPs) and GTPase exchange factors (GEFs), which regulate GTPase activity to induce cytoskeletal remodeling crucial for activity-dependent spine plasticity^{1,20,21}. PKC has been linked to actin regulation in many cell types. In neurons, application of phorbol esters, which activate PKC, can induce structural changes including growth cone retraction or collapse and the formation of lamellae in dendrites^{22,23}. These data suggest that PKC can regulate actin through modulating small GTPase function, however whether these pathways are involved during structural plasticity of spines and which small GTPases might be regulated are unknown²⁴.

Results

Here, we examine whether PKC α regulates small GTPases during the induction of plasticity.

¹Neuronal Signal Transduction Group, Max Planck Florida Institute for Neuroscience, Jupiter, FL, USA. ²International Max Planck Research School for Brain and Behavior, Jupiter, FL, USA. ³FAU/Max Planck Florida Institute Joint Graduate Program in Integrative Biology and Neuroscience, Florida Atlantic University, Boca Raton, FL, USA. *email: Ryohei.Yasuda@mpfi.org; Lesley.Colgan@mpfi.org

In order to study signaling in single spines during structural plasticity, we combined two-photon release of caged glutamate²⁵, fluorescence resonance energy transfer (FRET)-based sensors, and two-photon fluorescence lifetime imaging microscopy (2pFLIM)²⁶ to monitor the dynamics of intracellular signaling events with high spatiotemporal resolution. Specifically, using previously published FRET sensors, we monitored the spatiotemporal activation of the actin-regulating small GTPases, including Ras^{27–29}, Cdc42¹⁵ and Rac1¹⁹ during the induction of structural long-term potentiation (sLTP). Briefly, these sensors are composed of two components: (1) full length GTPase fused to green fluorescent protein (GTPase-eGFP), and (2) a specific GTPase binding domain of a downstream effector fused to two copies of red fluorescent protein (mRFP-effector-mRFP) (Fig. 1a). Activation of the GTPase increases the affinity between the two components of the sensor and the FRET between the fluorophores. Using 2pFLIM we can measure small GTPase activation by monitoring changes in the binding of the sensor components (binding fraction) through quantitatively measuring decreases in the fluorescence lifetime of GFP.

We transfected organotypic hippocampal slices from wildtype (WT) or PKC α knockout (KO) mice with small GTPase sensors and imaged CA1 pyramidal neurons using 2pFLIM. In response to glutamate uncaging targeted to a single dendritic spine (30 pulses at 0.5 Hz), the stimulated spine from WT slices rapidly enlarged by ~150% (transient phase) and persisted with an increased volume of ~40% (sustained phase) lasting at least 25 min (Fig. 1b,c). This sustained increase in the spine volume is highly correlated with increases in the functional strength of the stimulated spine^{28,30}. Consistent with previous work, hippocampal CA1 neurons from PKC α KO mice showed a deficit in sLTP¹⁴. Moreover, sLTP of stimulated spines expressing Rac1 sensor was consistent with spines expressing eGFP alone (Fig. 1c), demonstrating, and consistent with previous characterization^{15,19}, that effects of sensor overexpression on endogenous signaling are minimal. When sLTP was induced in single dendritic spines, we observed rapid and sustained activation of Rac1 (Fig. 1b,d) in the WT slices that was consistent with previously reported findings¹⁹. However, we found that in the absence of PKC α , Rac1 activity is lower at baseline and its activation is significantly attenuated during sLTP (Fig. 1d,e). Rac1 activity in WT mice was restricted to the stimulated spines at early time points (2–4 min), but spread into the dendrite and nearby spines at later time points (10–20 min), consistent with a previous study¹⁹. In PKC α KO mice, Rac1 activity in both stimulated spines and adjacent dendrites were attenuated (Fig. 1e,f). Thus, PKC α positively regulates Rac1 activation to facilitate plasticity.

In order to test the specificity of PKC α signaling toward Rac1, we tested whether the plasticity-induced activation of other small GTPases involved in plasticity, Ras or Cdc42^{1,31,32}, was also impaired in the absence of PKC α . Impairment of the functionally relevant sustained phase of sLTP was observed in PKC α KO neurons transfected with Ras or Cdc42 sensor (Fig. 2a,c). However, the activation of these two small GTPases during sLTP were not affected by loss of PKC α (Fig. 2b,d). This demonstrates that Rac1 but not Ras or Cdc42 is downstream of PKC α during sLTP.

We next investigated whether the PDZ binding domain of PKC α , which was shown to be critical for its isozyme-specific signaling in spine plasticity¹⁴, was required for downstream regulation of Rac1 (Fig. 3a). PKC α or PKC α lacking its PDZ binding domain was sparsely and postsynaptically expressed alongside the Rac1 sensor in hippocampal slices from PKC α KO mice. We found impairment of sLTP (Fig. 3b) and Rac1 activation (Fig. 3c) only when the PDZ binding domain was disrupted. This finding suggests a crucial role for PDZ binding domain of PKC α in Rac1 activation during sLTP.

Discussion

In this study, we have described that PKC α regulates the activation of Rac1, but not Ras or Cdc42, during sLTP of dendritic spines (Fig. 3d). This modulation relies on PKC α 's PDZ-binding motif, which may localize PKC α to a signaling complex scaffold that also recruits Rac1 GTPase-activating proteins (GAPs) or Guanine nucleotide-exchange factors (GEFs). Although the specific mechanism through which PKC α regulates Rac1 activity remains to be determined, potential scaffolds include PICK1, SAP-97 or PSD-95, which can interact with PKC α through its C-terminal PDZ binding domain and have been implicated in plasticity of spines^{33–38}.

The regulation of Rac1 during plasticity through GAPs and GEFs is highly complex in order to allow for tightly-regulated remodeling of various cytoskeletal domains in a precise spatial and temporal pattern³⁹. Rac1 has been shown to be localized to signaling complexes that scaffold upstream activators, small GTPases and downstream effectors, enabling subcompartmentalization of functional output⁴⁰. Rac1 activation promotes F-actin polymerization that facilitates spine growth and stabilization through the activation of major downstream targets p21-activated kinase (PAK), LIM kinase I (LIMKI) and WAVE regulatory complex (WRC)^{31,41}. The phosphorylation of PAK and LIMKI leads to inactivation of actin depolymerizing factor ADF/cofilin, which in turn stimulates F-actin polymerization^{1,31}. Additionally, Rac1 regulates actin branching through activation of WRC which drives Arp2/3^{41,42}. Interestingly, PICK1 has also been shown to bind and regulate Arp2/3⁴³.

While PKC α could modulate Rac1 through inhibition of a GAP or Rho GDP dissociation inhibitors (RhoGDIs)^{44–46}, much of the specificity of Rac1 GTPase signaling is reportedly regulated by GEFs^{46–48}. At least ten different RhoGEFs have been identified to be localized to the post-synaptic density⁴⁹. Of these, Kalirin 7, Tiam1 and B-Pix all show preferential GEF activity for Rac1, are able to be phosphorylated by classic PKC isozymes *in-vitro* and are required for sLTP of spines^{50–57}. Tiam1 contains a PDZ domain that could potentially interact with PKC α , however the structure of its PDZ domain does not predict PKC α as a preferred binding partner⁵⁸. Kalirin7 and B-Pix also each contain a PDZ binding domain, which could localize them to PDZ containing-scaffolds together with activated PKC α ^{57,59,60}. Indeed Kalirin-7 binds scaffolds including PSD-95, PICK1 and SAP97 *in vitro*. Only its interaction with PSD-95 has been confirmed in hippocampal neurons⁶¹.

It is important to note that these experiments rely on overexpression of small GTPase sensors. Importantly the effects of sensor overexpression on volume change of stimulated spines, sensor activation and kinetics have been well characterized and show minimal effects in WT neurons^{15,19,28}. However, as observed in Fig. 2c, PKC α KO animals did not have significantly impaired transient plasticity. Thus, it is possible that overexpression of

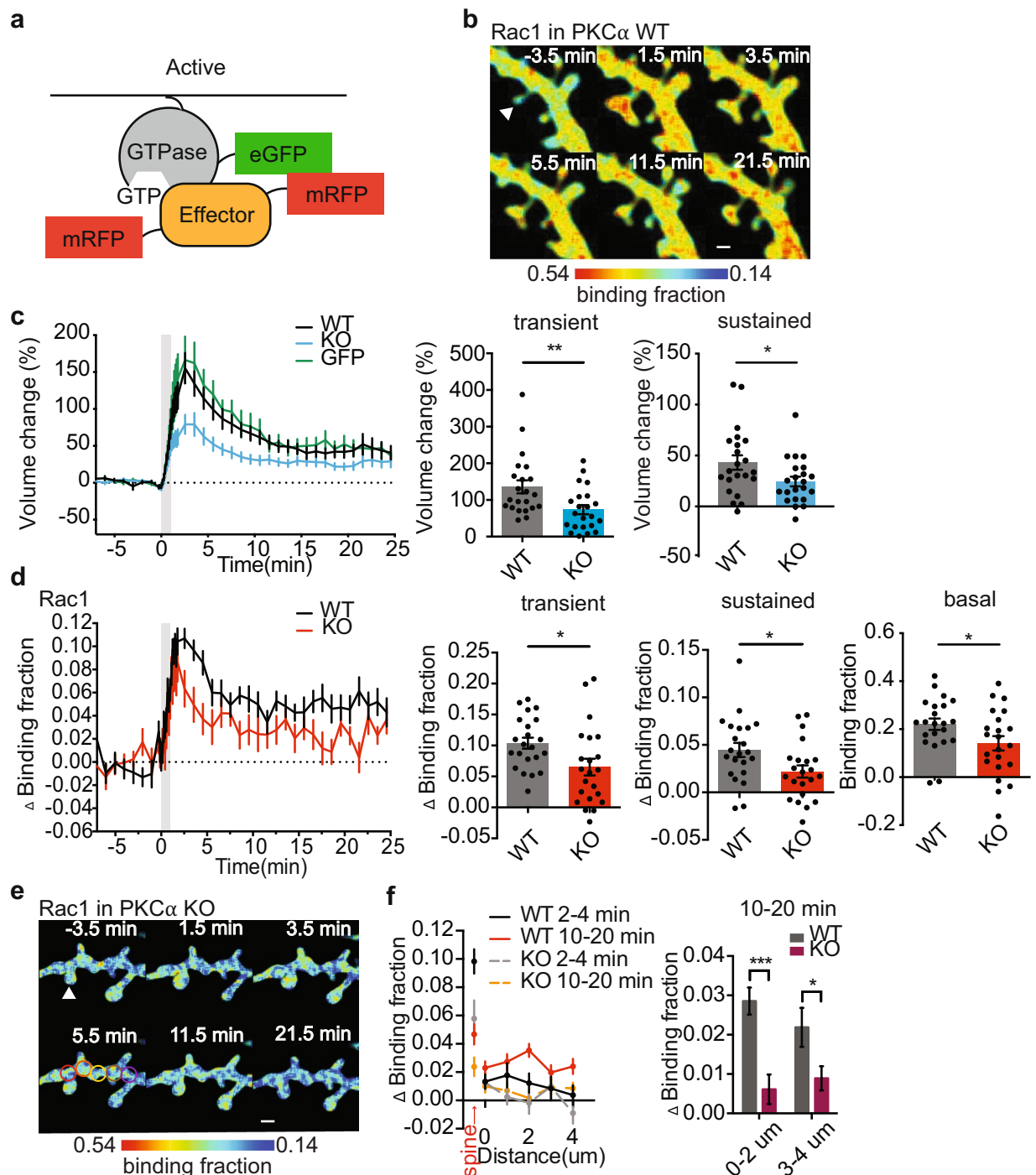


Figure 1. PKC regulates Rac1 activation during sLTP. **(a)** Schematic of small GTPase FRET sensors. **(b)** 2pFLIM images of Rac1 activation in WT slices at indicated time points. Arrowhead represents point of uncaging. Warmer colors indicate higher binding fraction of sensor and higher Rac1 activity. Scale bar, 1 μ m. **(c)** Time courses and quantification of transient (1–3 min) and sustained (10–25 min) spine volume change induced by glutamate uncaging in neurons expressing GFP or in neurons from PKC α WT and KO littermates expressing Rac1 sensor. **(d)** Time courses and quantification of transient (1.5–3.5 min), sustained (10–25 min) and basal (–8–0 min) Rac1 activation in stimulated spines from WT and PKC α KO littermates. **(e)** 2pFLIM images of Rac1 activation in PKC α KO slices at indicated time points. Arrowhead represents point of uncaging. Spreading of Rac1 activation in the dendrite were measured in the regions 0 μ m from the stimulated spine (red), 1 μ m (orange), 2 μ m (yellow), 3 μ m (brown) and 4 μ m (purple). Scale bar, 1 μ m. **(f)** Spatial profile and quantification of spreading Rac1 activation along the dendrite at indicated times and distances from the stimulated spine in WT and PKC α KO littermates. Data are mean \pm s.e.m. Grey shading indicates time of uncaging. * $P < 0.05$, ** $P < 0.01$ two-tailed t-test (**c,d**) and two-way ANOVA with Sidak's multiple comparisons test (**f**). n (neurons/spines) = 18/22 WT, 19/22 PKC α KO and 5/11 GFP.

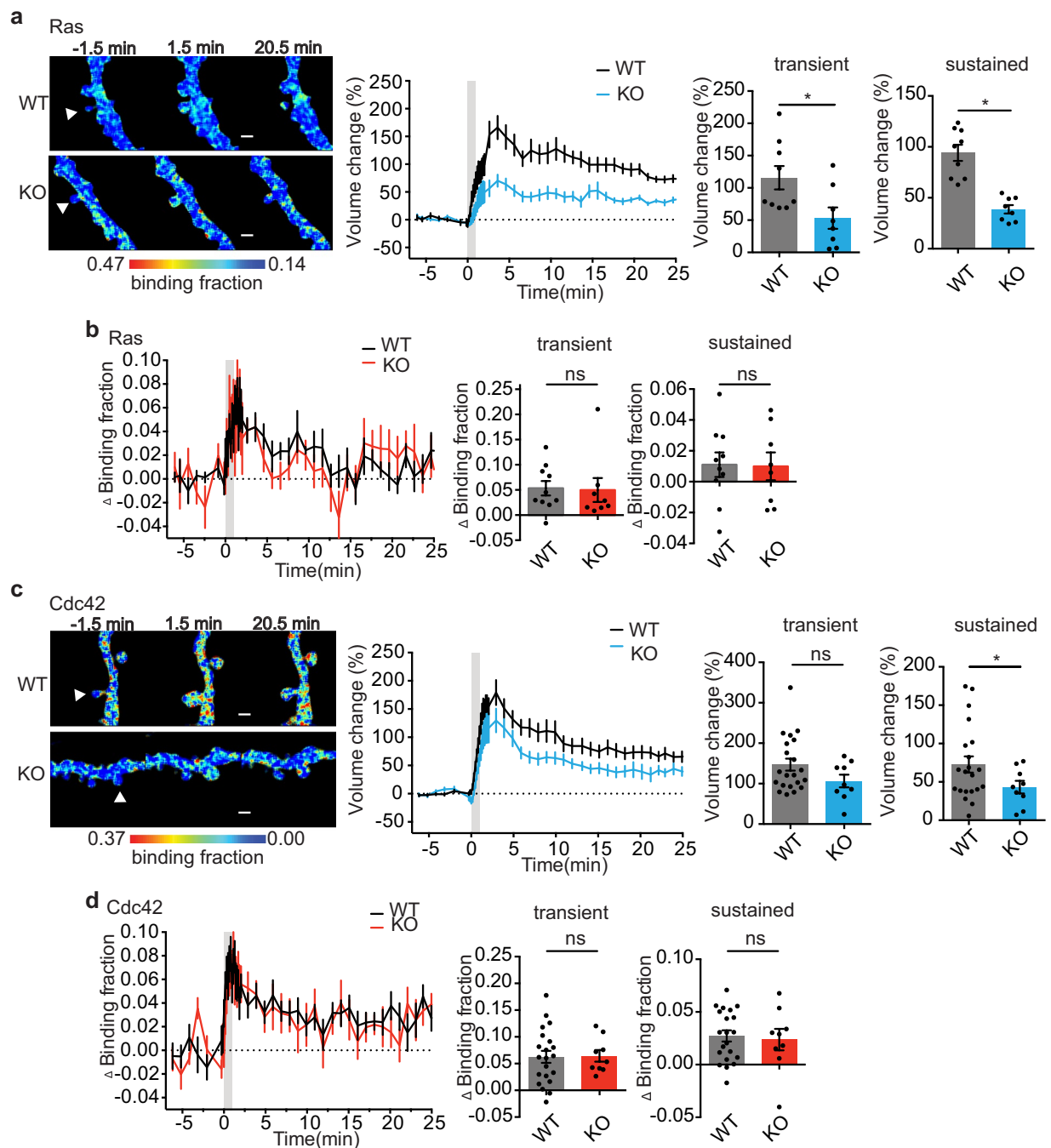


Figure 2. PKC α does not regulate Ras or Cdc42 activation during sLTP. **(a,c)** 2pFLIM images of Ras **(a)** and Cdc42 **(c)** activation in PKC α WT and KO neurons at indicated time points. Time courses and quantification of transient (1–3 min) and sustained (10–25 min) spine volume change induced by glutamate uncaging in neurons expressing Ras1 sensor **(a)** or Cdc42 sensor **(c)** from PKC α WT and KO littermates. **(b,d)** Time courses and quantification of transient (1–3 min) and sustained (10–25 min) Ras1 **(b)** or Cdc42 **(d)** activation in stimulated spines from WT and PKC α KO littermates. Data are mean \pm s.e.m. n(neurons/spines) Ras: n = 8/10 WT, n = 7/8 KO. Cdc42: n = 15/21 WT and n = 7/9 KO *P < 0.05, two-tailed t-test.

Cdc42 may partially rescue the impairment of plasticity in a KO background. This finding is interesting given the known crosstalk between Cdc42 and Rac1 in regulating actin dynamics⁶². Rac1 and Cdc42 share several common effectors⁶³ that are relevant to structural plasticity of spines. For example, both activated Rac and Cdc42 can increase PAK1 association with LIMK and LIMK-dependent phosphorylation of cofilin⁶⁴. Cofilin phosphorylation has been shown to be an important regulator of actin remodeling during structural plasticity of spines and is transiently increased during the early phase (~2 min) of plasticity⁶⁵. Thus, overexpression of Cdc42 may alleviate

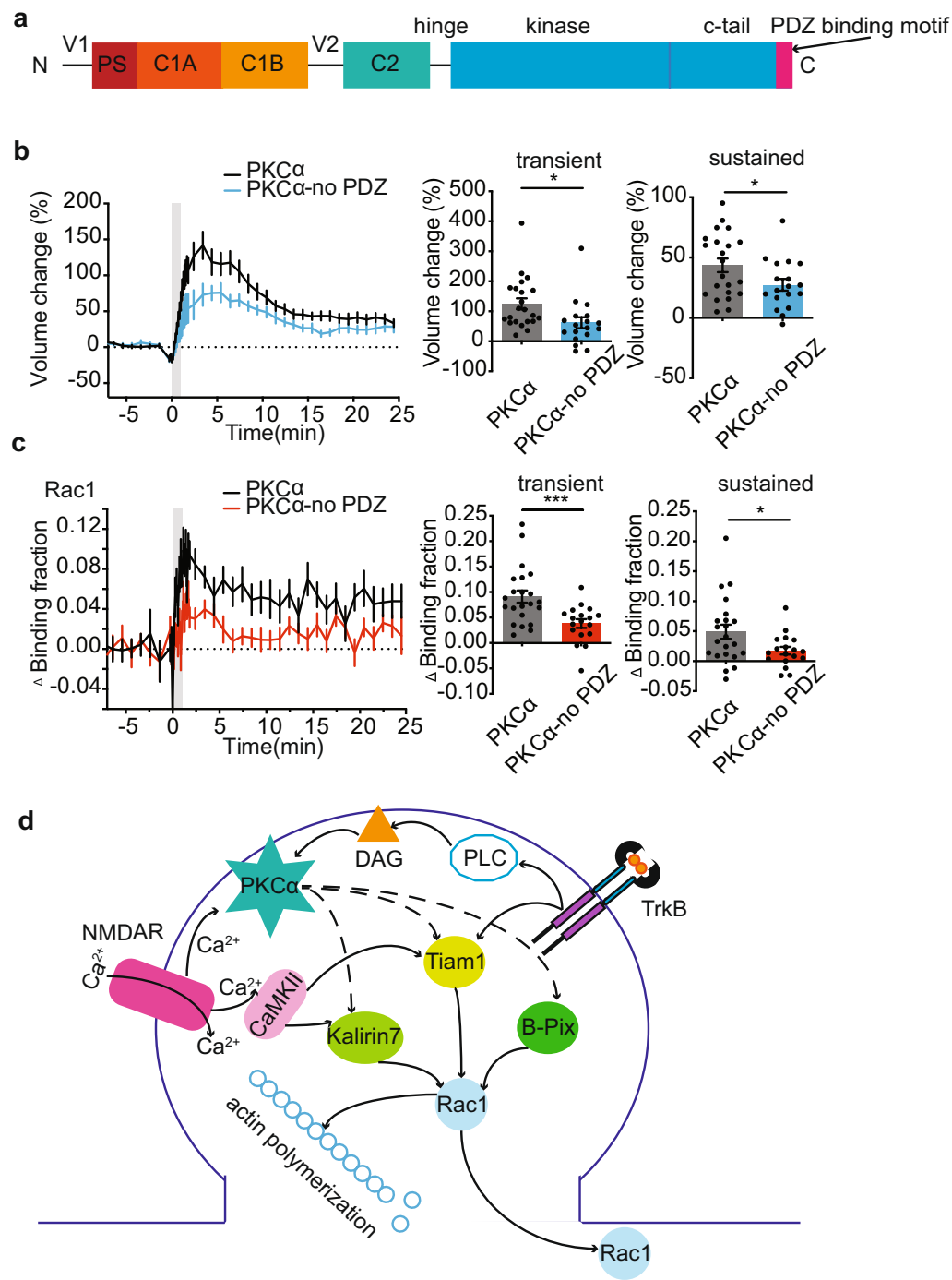


Figure 3. PKC α regulates Rac1 activation during sLTP via PDZ binding domain. **(a)** Primary structure of PKC α showing pseudosubstrate, C1A and C1B domains, C2 domain, kinase domain, C-terminal tail, and PDZ binding motif. **(b,c)** Time courses and quantification of transient (1–3 min) and sustained (10–25 min) spine volume change **(b)** and transient and sustained Rac1 activation **(c)** induced by glutamate uncaging in PKC α KO hippocampal neurons expressing PKC α or PKC α without PDZ domain (PKC α -no PDZ). $n = 20/22$ PKC α and $14/18$ PKC α -no PDZ (neurons/spines). Data are mean \pm s.e.m. * $P < 0.05$, two-tailed t-test. **(d)** Schematic of potential PKC α regulation of Rac1.

some of the PKC α – Rac1 mediated KO deficits. Further study on potential crosstalk between Cdc42 and Rac1, particularly related to cofilin regulation during structural plasticity of spines will be informative.

Both Rac1 and PKC α activation are downstream of TrkB receptor activation in the stimulated spine^{14,19} (Fig. 3d). One important future direction is to determine if TrkB-dependent activation of Rac1 is solely through PKC α or whether a more complex feedback loop is in play. The increased activity and spreading of Rac1 promoted by PKC α is consistent with an essential role for PKC α in integrating neurotrophic signals to facilitate plasticity. Moreover, this link between PKC α and Rac1 supports a growing understanding of the molecular mechanisms underlying heterosynaptic facilitation, whereby the induction of plasticity in one spine lowers the threshold of plasticity induction in nearby spines^{14,28,66}.

This study identified a novel molecular pathway that links short-lived calcium influx and activation of PKC α , to long-lasting Rac1 activation and changes in spine structure. This work, taken together with previous findings that another Ca²⁺-dependent kinase, CaMKII, also activates Rac1 during sLTP^{57,66}, Rac1 appears to be a key convergence point of multiple upstream calcium-dependent pathways (Fig. 3d). We anticipate that the better understanding of Rac1 signaling pathway may ultimately help us to uncover the signaling network with which memories are encoded.

Materials and Methods

Animals. All experimental procedures were approved and carried out in accordance to the regulations of the Max Planck Florida Institute for Neuroscience Animal Care and Use Committee in accordance with guidelines by the US National Institutes of Health. P4–P8 mouse pups from both sexes were used for organotypic slices for imaging studies. The genotype of each animal was verified before preparing slices. PKC α KO 129/sv animals were received from Dr. Michael Leitges. Animals were crossed to C57Bl/6N Crl and are on a mixed background. For all the experiments, WT littermates were used as controls for KO animals.

Plasmids. All the plasmids used were previously developed and described in publication and are available on Addgene^{14,19,67}. Briefly, the Rac1 sensor consisted of mEGFP-Rac1 (Addgene #83950) and mCherry-PAK2 binding domain-mCherry (Addgene #83951), the Ras sensor consisted of pCI-mEGFP-HRas ((Addgene #18666) and pCI-mRFP-RBD^{K65E,K108A}-mRFP (Addgene #45149), the Cdc42 sensor consisted of mEGFP-Cdc42 (Addgene #29673) and mCherry-Pak3(60-113)/S74A/F84A-mCherry-C1 (Addgene #29676). PKC α (*Bos taurus*) was cloned into CMV-promoter-containing mEGFP C1 vectors such that mEGFP was fused to the N terminus of PKC α ¹⁴. mEGFP-PKC α Δ QSAV was made by introducing a single point mutation into mEGFP-PKC α /C1 to introduce a stop codon before the last four amino acids (QSAV) of PKC α ¹⁴.

Organotypic hippocampal slice cultures and transfection. Organotypic hippocampal slices were prepared from wildtype or transgenic postnatal 4–8 day old mouse pups of both sexes as previously described⁶⁸. In brief, the animals were anaesthetized with isoflurane, after which the animal was quickly decapitated and the brain removed. The hippocampi were dissected and cut into 350 μ m thick coronal hippocampal slices using a McIlwain tissue chopper (Ted Pella, Inc) and plated on hydrophilic PTFE membranes (Millicell, Millipore) fed by culture medium containing MEM medium (Life Technologies), 20% horse serum, 1mM L-Glutamine, 1 mM CaCl₂, 2 mM MgSO₄, 12.9 mM D-Glucose, 5.2 mM NaHCO₃, 30 mM Hepes, 0.075% Ascorbic Acid, 1 μ g/ml Insulin. Slices were incubated at 37 °C in 5% CO₂. After 7–12 days in culture, CA1 pyramidal neurons were transfected with biolistic gene transfer⁶⁹ using 1.0 μ m gold beads (8–12 mg) coated with plasmids containing 50 μ g of total cDNA of interest in the following ratios. Rac1 sensor, donor: acceptor = 1:2; Rac1 sensor plus PKC α , donor: acceptor: PKC α = 1:2:1; Rac1 sensor plus PKC α without PDZ binding domain, donor: acceptor: PKC α - no PDZ domain = 1:2:1; Ras sensor, donor: acceptor = 1:3; Cdc42 sensor, donor: acceptor = 1:1). Neurons expressing all plasmid combinations were imaged 2–5 days after transfection.

2pFLIM. FLIM imaging using a custom-built two-photon fluorescence lifetime imaging microscope was performed as previously described¹⁵. 2pFLIM imaging was performed using a Ti-sapphire laser (Coherent, Cameleon) at a wavelength of 920 nm with a power of 1.4–1.6 mW. Fluorescence emission was collected using an immersion objective (60 \times , numerical aperture 0.9, Olympus), divided with a dichroic mirror (565 nm) and detected with two separated photoelectron multiplier tubes placed after wavelength filters (Chroma, 510/70-2p for green and 620/90-2p for red). Both red and green channels were fit with photoelectron multiplier tubes (PMT) having a low transfer time spread (H7422-40p; Hamamatsu) to allow for fluorescence lifetime imaging. Photon counting for fluorescence lifetime imaging was performed using a time-correlated single photon counting board (SPC-150; Becker and Hickl) and fluorescence images were acquired with PCI-6110 (National instrument) using modified ScanImage⁷⁰ (https://github.com/ryoheiyasuda/FLIMimage_Matlab_ScanImage). Intensity images for analysis of sLTP volume changes were collected by 128 \times 128 pixels as a z stack of three slices with 1 μ m separation and averaging 6 frames/slice. Spine volume was measured as the integrated fluorescent intensity of EGFP after subtracting background (F). Spine volume change was calculated by F/F₀, in which F₀ is the average spine intensity before stimulation.

Two-photon glutamate uncaging. A second Ti-sapphire laser tuned at a wavelength of 720 nm was used to uncage 4-methoxy-7-nitroindolyl-caged-L-glutamate (MNI-caged glutamate) in extracellular solution with a train of 4–8 ms, 2.8–3.0 mW pulses (30 times at 0.5 Hz) in a small region \sim 0.5 μ m from the spine of interest as previously described¹⁴. Experiments were performed in Mg²⁺ free artificial cerebral spinal fluid (ACSF; 127 mM NaCl, 2.5 mM KCl, 4 mM CaCl₂, 25 mM NaHCO₃, 1.25 mM NaH₂PO₄ and 25 mM glucose) containing 1 μ M tetrodotoxin (TTX) and 4 mM MNI-caged L-glutamate aerated with 95% O₂ and 5% CO₂. Experiments were performed at room temperature.

2pFLIM analysis. To measure the fraction of donor that was undergoing FRET with acceptor (Binding Fraction), we fit a fluorescence lifetime curve summing all pixels over a whole image with a double exponential function convolved with the Gaussian pulse response function:

$$F(t) = F_0[P_D H(t, t_0, \tau_D, \tau_G) + P_{AD} H(t, t_0, \tau_{AD}, \tau_G)]$$

where τ_{AD} is the fluorescence lifetime of donor bound with acceptor, P_D and P_{AD} are the fraction of free donor and donor undergoing FRET with acceptor, respectively, and $H(t)$ is a fluorescence lifetime curve with a single exponential function convolved with the Gaussian pulse response function:

$$H(t, t_0, \tau_D, \tau_G) = \frac{1}{2} \exp\left(\frac{\tau_G^2}{2\tau_D^2} - \frac{t - t_0}{\tau_D}\right) \operatorname{erfc}\left(\frac{\tau_G^2 - \tau_D(t - t_0)}{\sqrt{2\tau_D\tau_G}}\right),$$

in which τ_D is the fluorescence lifetime of the free donor, τ_G is the width of the Gaussian pulse response function, F_0 is the peak fluorescence before convolution and t_0 is the time offset, and erfc is the complementary error function.

We fixed τ_D to the fluorescence lifetime obtained from free eGFP (2.6 ns), and then fixed τ_{AD} to fluorescence lifetime of the donor bound with acceptor (1.1 ns). For experimental data, we fixed τ_D and τ_{AD} to these values to obtain stable fitting.

To generate the fluorescence lifetime image, we calculated the mean photon arrival time, $\langle t \rangle$, in each pixel as:

$$\langle t \rangle = \int tF(t)dt / \int F(t)dt,$$

Then, the mean photon arrival time is related to the mean fluorescence lifetime, $\langle \tau \rangle$, by an offset arrival time, t_0 , which is obtained by fitting the whole image:

$$\langle T \rangle = \langle t \rangle - t_0.$$

For small regions-of-interest (ROIs) in an image (spines or dendrites), we calculated the binding fraction (P_{AD}) as:

$$P_{AD} = \tau_D(T_D - \langle T \rangle)(T_D - T_{AD})^{-1}(T_D + T_{AD} - \langle T \rangle)^{-1}.$$

Data with lifetime fluctuations in the baseline that were greater than 0.15 ns were excluded before further analysis. To analyse the spatial spreading of Rac1 activation, contiguous 1 μm diameter ROIs along dendrite from the base of the stimulated spines were analysed for Rac1 activation over time.

Statistical analysis. All values are presented as mean \pm SEM unless otherwise noted. Number of independent measurements (n [neurons/spines]) is indicated in figure legends. Unpaired two-tailed student's t test was used for comparing two independent samples. Two-way ANOVA followed by multiple comparison test was used to compare grouped data sets (Prism 6, GraphPad). Data were excluded if obvious signs of poor cellular health (for example, dendritic blebbing, spine collapse) were apparent. In addition, outlier analysis was performed on spine volume data with ROUT ($Q = 1\%$). This analysis led to the exclusion of 2 out of 113 spines from analysis.

Received: 15 September 2019; Accepted: 17 January 2020;

Published online: 04 February 2020

References

- Lai, K.-O. & Ip, N. Y. Structural plasticity of dendritic spines: The underlying mechanisms and its dysregulation in brain disorders. *Biochim. Biophys. Acta - Mol. Basis Dis.* **1832**, 2257–2263 (2013).
- Lamprecht, R. & LeDoux, J. Structural plasticity and memory. *Nat. Rev. Neurosci.* **5**, 45–54 (2004).
- Hayashi-Takagi, A. *et al.* Labelling and optical erasure of synaptic memory traces in the motor cortex. *Nature*, **525**(7569), 333–338 (2015).
- Nishiyama, J. & Yasuda, R. Biochemical Computation for Spine Structural Plasticity. *Neuron* **87**, 63–75 (2015).
- Kennedy, M. B. Synaptic Signaling in Learning and Memory. *Cold Spring Harb. Perspect. Biol.* **8**, a016824 (2016).
- Malinow, R., Madison, D. V. & Tsien, R. W. Persistent protein kinase activity underlying long-term potentiation. *Nature* **335**, 820–824 (1988).
- Malinow, R., Schulman, H. & Tsien, R. W. Inhibition of postsynaptic PKC or CaMKII blocks induction but not expression of LTP. *Science* **245**, 862–6 (1989).
- Hu, G.-Y. *et al.* Protein kinase C injection into hippocampal pyramidal cells elicits features of long term potentiation. *Nature* **328**, 426–429 (1987).
- Zhang, G.-R. *et al.* Genetic enhancement of visual learning by activation of protein kinase C pathways in small groups of rat cortical neurons. *J. Neurosci.* **25**, 8468–81 (2005).
- Clark, E. A., Leach, K. L., Trojanowski, J. Q. & Lee, V. M. Characterization and differential distribution of the three major human protein kinase C isozymes (PKC alpha, PKC beta, and PKC gamma) of the central nervous system in normal and Alzheimer's disease brains. *Lab. Invest.* **64**, 35–44 (1991).
- Ito, A. *et al.* Immunocytochemical localization of the alpha subspecies of protein kinase C in rat brain. *Proc. Natl. Acad. Sci. USA* **87**, 3195–9 (1990).
- Kose, A., Ito, A., Saito, N. & Tanaka, C. Electron microscopic localization of gamma- and beta II-subspecies of protein kinase C in rat hippocampus. *Brain Res.* **518**, 209–17 (1990).
- Sossin, W. S. Isoform specificity of protein kinase Cs in synaptic plasticity. *Learn. Mem.* **14**, 236–246 (2007).
- Colgan, L. A. *et al.* PKC α integrates spatiotemporally distinct Ca $^{2+}$ and autocrine BDNF signaling to facilitate synaptic plasticity. *Nat. Neurosci.* **21**, 1027–1037 (2018).

15. Murakoshi, H., Wang, H. & Yasuda, R. Local, persistent activation of Rho GTPases during plasticity of single dendritic spines. *Nature* **472**, 100–4 (2011).
16. Kim, I. H., Wang, H., Soderling, S. H. & Yasuda, R. Loss of Cdc42 leads to defects in synaptic plasticity and remote memory recall. *Elife* **3** (2014).
17. Bailey, C. H., Kandel, E. R. & Harris, K. M. Structural Components of Synaptic Plasticity and Memory Consolidation. *Cold Spring Harb Perspect Biol* **7** (2015).
18. Patterson, M. & Yasuda, R. Signalling pathways underlying structural plasticity of dendritic spines. *Br J Pharmacol* **163**, 1626–1638 (2011).
19. Hedrick, N. G. *et al.* Rho GTPase complementation underlies BDNF-dependent homo- and heterosynaptic plasticity. *Nature*, <https://doi.org/10.1038/nature19784> (2016).
20. Govek, E.-E., Newey, S. E. & Van Aelst, L. The role of the Rho GTPases in neuronal development. *Genes Dev.* **19**, 1–49 (2005).
21. Saneyoshi, T. *et al.* Activity-dependent synaptogenesis: regulation by a CaM-kinase kinase/CaM-kinase I/betaPIX signaling complex. *Neuron* **57**, 94–107 (2008).
22. Pipel, Y. & Segal, M. Activation of PKC induces rapid morphological plasticity in dendrites of hippocampal neurons via Rac and Rho-dependent mechanisms. *Eur. J. Neurosci.* **19**, 3151–3164 (2004).
23. Yang, Q. *et al.* Protein kinase C activation decreases peripheral actin network density and increases central nonmuscle myosin II contractility in neuronal growth cones. *Mol. Biol. Cell* **24**, 3097–3114 (2013).
24. Brandt, D., Gimona, M., Hillmann, M., Haller, H. & Mischak, H. Protein kinase C induces actin reorganization via a Src- and Rho-dependent pathway. *J. Biol. Chem.* **277**, 20903–20910 (2002).
25. Matsuzaki, M. *et al.* Dendritic spine geometry is critical for AMPA receptor expression in hippocampal CA1 pyramidal neurons. *Nat. Neurosci.* **4**, 1086–1092 (2001).
26. Yasuda, R. Imaging intracellular signaling using two-photon fluorescent lifetime imaging microscopy. *Cold Spring Harb Protoc.* **2012**, 1121–1128 (2012).
27. Oliveira, A. F. & Yasuda, R. Imaging the activity of Ras superfamily GTPase proteins in small subcellular compartments in neurons. *Methods Mol Biol* **1071**, 109–128 (2014).
28. Harvey, C. D., Yasuda, R., Zhong, H. & Svoboda, K. The spread of Ras activity triggered by activation of a single dendritic spine. *Science* **321**, 136–40 (2008).
29. Yasuda, R. *et al.* Supersensitive Ras activation in dendrites and spines revealed by two-photon fluorescence lifetime imaging. *Nat. Neurosci.* **9**, 283–291 (2006).
30. Matsuzaki, M., Honkura, N., Ellis-Davies, G. C. & Kasai, H. Structural basis of long-term potentiation in single dendritic spines. *Nature* **429**, 761–766 (2004).
31. Sit, S.-T. & Manser, E. Rho GTPases and their role in organizing the actin cytoskeleton. *J. Cell Sci.* **124**, 679–683 (2011).
32. Zhu, J. J., Qin, Y., Zhao, M., Van Aelst, L. & Malinow, R. Ras and Rap Control AMPA Receptor Trafficking during Synaptic Plasticity. *Cell* **110**, 443–455 (2002).
33. Callender, J. A. & Newton, A. C. Conventional protein kinase C in the brain: 40 years later. *Neuronal Signal.* **1**, NS20160005 (2017).
34. Ehrlich, I., Klein, M., Rumpel, S. & Malinow, R. PSD-95 is required for activity-driven synapse stabilization. *Proc. Natl. Acad. Sci. USA* **104**, 4176–81 (2007).
35. Nakamura, Y. *et al.* PICK1 inhibition of the Arp2/3 complex controls dendritic spine size and synaptic plasticity. *EMBO J.* **30**, 719–30 (2011).
36. Staudinger, J., Lu, J. & Olson, E. N. Specific interaction of the PDZ domain protein PICK1 with the COOH terminus of protein kinase C- α . *J. Biol. Chem.* **272**, 32019–24 (1997).
37. Volk, L., Kim, C.-H., Takamiya, K., Yu, Y. & Huganir, R. L. Developmental regulation of protein interacting with C kinase 1 (PICK1) function in hippocampal synaptic plasticity and learning. *Proc. Natl. Acad. Sci. USA* **107**, 21784–9 (2010).
38. Waites, C. L. *et al.* Synaptic SAP97 isoforms regulate AMPA receptor dynamics and access to presynaptic glutamate. *J. Neurosci.* **29**, 4332–45 (2009).
39. Woolfrey, K. M. & Srivastava, D. P. Control of Dendritic Spine Morphological and Functional Plasticity by Small GTPases. *Neural Plasticity* **2016** (2016).
40. Colgan, L. A. & Yasuda, R. Plasticity of dendritic spines: subcompartmentalization of signaling. *Annu Rev Physiol* **76**, 365–385 (2014).
41. Spence, E. F. & Soderling, S. H. Actin out: Regulation of the synaptic cytoskeleton. *Journal of Biological Chemistry* **290**, 28613–28622 (2015).
42. Chen, B. *et al.* Rac1 GTPase activates the WAVE regulatory complex through two distinct binding sites. *Elife* **6** (2017).
43. Rocca, D. L., Martin, S., Jenkins, E. L. & Hanley, J. G. Inhibition of Arp2/3-mediated actin polymerization by PICK1 regulates neuronal morphology and AMPA receptor endocytosis. *Nat. Cell Biol.* **10**, 259–271 (2008).
44. Zhang, B., Chernoff, J. & Zheng, Y. Interaction of Rac1 with GTPase-activating proteins and putative effectors. A comparison with Cdc42 and RhoA. *J. Biol. Chem.* **273**, 8776–8782 (1998).
45. Garcia-Mata, R., Boulter, E. & Burridge, K. The ‘invisible hand’: regulation of RHO GTPases by RHOGDIs. *Nat. Publ. Gr.* **12**, 493 (2011).
46. Van Aelst, L. & D’Souza-Schorey, C. Rho GTPases and signaling networks. *Genes Dev.* **11**, 2295–322 (1997).
47. Cook, D. R., Rossman, K. L. & Der, C. J. Rho guanine nucleotide exchange factors: regulators of Rho GTPase activity in development and disease. *Oncogene* **33**, 4021–35 (2014).
48. Bellanger, J.-M. *et al.* The Rac1- and RhoG-specific GEF domain of Trio targets filamin to remodel cytoskeletal actin. *Nat. Cell Biol.* **2**, 888–892 (2000).
49. Kiraly, D. D., Eipper-Mains, J. E., Mains, R. E. & Eipper, B. A. Synaptic plasticity, a symphony in GEF. *ACS Chem. Neurosci.* **1**, 348–365 (2010).
50. Buchanan, F. G., Elliot, C. M., Gibbs, M. & Exton, J. H. Translocation of the Rac1 guanine nucleotide exchange factor Tiam1 induced by platelet-derived growth factor and lysophosphatidic acid. *J. Biol. Chem.* **275**, 9742–8 (2000).
51. Chen, J.-Y., Lin, Y.-Y. & Jou, T.-S. Phosphorylation of EBP50 negatively regulates β -PIX-dependent Rac1 activity in anoikis. *Cell Death Differ.* **19**, 1027–37 (2012).
52. Fleming, I. N., Elliott, C. M., Buchanan, F. G., Downes, C. P. & Exton, J. H. Ca²⁺/calmodulin-dependent protein kinase II regulates Tiam1 by reversible protein phosphorylation. *J. Biol. Chem.* **274**, 12753–8 (1999).
53. Fleming, I. N., Elliott, C. M., Collard, J. G. & Exton, J. H. Lysophosphatidic Acid Induces Threonine Phosphorylation of Tiam1 in Swiss 3T3 Fibroblasts via Activation of Protein Kinase C. *J. Biol. Chem.* **272**, 33105–33110 (1997).
54. Mandela, P. & Ma, X.-M. Kalirin, a Key Player in Synapse Formation, Is Implicated in Human Diseases. *Neural Plast.* **2012**, 1–9 (2012).
55. Mertens, A. E., Roovers, R. C. & Collard, J. G. Regulation of Tiam1-Rac signalling. *FEBS Lett.* **546**, 11–16 (2003).
56. Shirafuji, T. *et al.* The role of Pak-interacting exchange factor- β phosphorylation at serines 340 and 583 by PKC γ in dopamine release. *J. Neurosci.* **34**, 9268–80 (2014).
57. Saneyoshi, T. *et al.* Reciprocal Activation within a Kinase-Effector Complex Underlying Persistence of Structural LTP. *Neuron* **102**, 1199–1210.e6 (2019).

58. Shepherd, T. R. *et al.* The Tiam1 PDZ Domain Couples to Syndecan1 and Promotes Cell–Matrix Adhesion. *J. Mol. Biol.* **398**, 730–746 (2010).
59. Penzes, P. *et al.* The Neuronal Rho-GEF Kalirin-7 Interacts with PDZ Domain–Containing Proteins and Regulates Dendritic Morphogenesis. *Neuron* **29**, 229–242 (2001).
60. Park, E. *et al.* The Shank family of postsynaptic density proteins interacts with and promotes synaptic accumulation of the beta PIX guanine nucleotide exchange factor for Rac1 and Cdc42. *J. Biol. Chem.* **278**, 19220–9 (2003).
61. Penzes, P. *et al.* The neuronal Rho-GEF Kalirin-7 interacts with PDZ domain-containing proteins and regulates dendritic morphogenesis. *Neuron* **29**, 229–242 (2001).
62. Guilluy, C., Garcia-Mata, R. & Burridge, K. Rho protein crosstalk: another social network? *Trends Cell Biol.* **21**, 718–726 (2011).
63. Bustelo, X. R., Sauzeau, V. & Berenjeno, I. M. GTP-binding proteins of the Rho/Rac family: Regulation, effectors and functions *in vivo*. *BioEssays* **29**, 356–370 (2007).
64. Edwards, D. C., Sanders, L. C., Bokoch, G. M. & Gill, G. N. Activation of LIM-kinase by Pak1 couples Rac/Cdc42 GTPase signalling to actin cytoskeletal dynamics. *Nat. Cell Biol.* **1**, 253–259 (1999).
65. Chen, L. Y., Rex, C. S., Casale, M. S., Gall, C. M. & Lynch, G. Changes in synaptic morphology accompany actin signaling during LTP. *J. Neurosci.* **27**, 5363–5372 (2007).
66. Hedrick, N. G. *et al.* Rho GTPase complementation underlies BDNF-dependent homo- and heterosynaptic plasticity. *Nature advance on* (2016).
67. Oliveira, A. F. & Yasuda, R. An improved Ras sensor for highly sensitive and quantitative FRET-FLIM imaging. *PLoS One* **8**, e52874 (2013).
68. Stoppini, L., Buchs, P.-A. & Müller, D. A simple method for organotypic cultures of nervous tissue. *J. Neurosci. Methods* **37**, 173–182 (1991).
69. O'Brien, J. A. & Lummis, S. C. R. Biolistic transfection of neuronal cultures using a hand-held gene gun. *Nat. Protoc.* **1**, 977–81 (2006).
70. Pologruto, T. A., Sabatini, B. L. & Svoboda, K. ScanImage: Flexible software for operating laser scanning microscopes. *Biomed. Eng. Online* **2**, 13 (2003).

Acknowledgements

We would like to thank Dr. Michael Leitges for the PKC α KO 129/sv animals; M. Dowdy, E. Garcia and the MPFI ARC for animal care; members of the Yasuda laboratory for discussion; L. Yan for helping with the microscope; and D. Kloetzer for managing the laboratory. This work was funded by NIH (R01MH080047 (RY), DP1NS096787 (RY), F32MH101954 (LAC)), Louis D Srybnik Foundation Inc. & Foundation for the Art, Science, and Education Inc, Brain Research Foundation and the Max Planck Florida Institute for Neuroscience.

Author contributions

Xun Tu: Conceptualization, Designed the experiments, Data curation, Formal analysis, Validation, Investigation, Visualization, Writing—original draft, Writing—review and editing. Ryohei Yasuda: Conceptualization, Supervision, Designed the experiments, Writing—review and editing. Lesley A Colgan: Conceptualization, Supervision, Investigation, Designed the experiments, Writing—review and editing.

Competing interests

Ryohei Yasuda is a founder and a share holder of Florida Lifetime Imaging LLC, a company that helps people set up FLIM.

Additional information

Correspondence and requests for materials should be addressed to R.Y. or L.A.C.

Reprints and permissions information is available at www.nature.com/reprints.

Publisher's note Springer Nature remains neutral with regard to jurisdictional claims in published maps and institutional affiliations.



Open Access This article is licensed under a Creative Commons Attribution 4.0 International License, which permits use, sharing, adaptation, distribution and reproduction in any medium or format, as long as you give appropriate credit to the original author(s) and the source, provide a link to the Creative Commons license, and indicate if changes were made. The images or other third party material in this article are included in the article's Creative Commons license, unless indicated otherwise in a credit line to the material. If material is not included in the article's Creative Commons license and your intended use is not permitted by statutory regulation or exceeds the permitted use, you will need to obtain permission directly from the copyright holder. To view a copy of this license, visit <http://creativecommons.org/licenses/by/4.0/>.

© The Author(s) 2020